DOI: 10.1002/ejic.200600554

Complexation of Uranium(VI) with Thiodiacetic Acid in Solution at 10–85 °C

Plinio Di Bernardo,*[a] PierLuigi Zanonato,[a] Arturo Bismondo,[b] Huijian Jiang,[c] Alexander Yu. Garnov,[c] Jun Jiang,[c] and Linfeng Rao*[c]

Keywords: Uranium / Thermodynamics / Carboxylate ligands / EXAFS spectroscopy / Temperature effect

The protonation of thiodiacetate and its complexation with uranium(VI) in 1.05 mol kg^{-1} $NaClO_4$ are studied at variable temperatures (10–85 °C). Three U^{VI} complexes (UO_2L, UO_2HL^+, and $UO_2HL_2^-$, where L is thiodiacetate) are identified in this temperature range. The formation constants and the enthalpies of complexation are determined by potentiometry and calorimetry. The complexation of uranium(VI) with thiodiacetate becomes more endothermic at higher temperatures. However, the complexes become stronger due to increasingly more positive entropies of complexation at higher temperatures, which exceeds the increase in the unfavorable enthalpy of complexation. The values of the heat capacity of complexation ($\Delta C_p°$) are 122 ± 16, 302 ± 26, and 242 ± 23 J K^{-1} mol^{-1} for UO_2L, UO_2HL^+, and $UO_2HL_2^-$, respectively. The effect of temperature on the thermodynamics of the complexation is discussed in terms of the electrostatic model and the change in the solvent structure.

Introduction

There has been significant interest in studies of the complexation of actinides with organic materials in solution at elevated temperatures due to the demand for scientific information to aid the safe management of nuclear wastes. The temperature of nuclear wastes in the storage tanks and the vicinity of the waste repository is known or estimated to be significantly above ambient temperature. For example, the temperature in the storage tanks is up to 90 °C and the temperature in the nuclear waste repository could be close to 100 °C thousands of years after the closure of the repository. Failure of the engineering barriers of the waste form could result in the contact of nuclear wastes with groundwater and possible migration of actinides into the environment. Prediction of the chemical behavior of actinides in waste processing and in the repository requires thermodynamic data on the complexation of actinides at elevated temperatures. At present, the majority of the thermodynamic data on actinide complexation are obtained at or near 25 °C.[1] The lack of data at elevated temperatures therefore makes it difficult to predict the behavior of actinides in waste processing and disposal, where elevated temperatures are expected.

While providing data to support the safe management of nuclear wastes, studies of the complexation of actinides at elevated temperatures could improve the fundamental understanding of the coordination chemistry of actinides as well. For example, the change in temperature perturbs the structure of solvent in the bulk and in the vicinity of the ions, alters its dielectric property, and thus affects the energetics of the complexation.[2,3] Therefore, the trends in thermodynamic parameters over a wide range of temperature could provide insight into the nature of the actinide complex and the solvent effect.

The liquid nuclear wastes in storage tanks are complex in composition and extremely diverse in acidity/basicity, ranging from strongly acidic to highly basic solutions. Many ligands could affect the behavior of actinides in liquid nuclear wastes by forming complexes. We have studied a series of mono- and dicarboxylic acids at elevated temperatures, including acetic,[4–7] malonic,[8] and oxydiacetic[9] acids. Some of the ligands exist in the nuclear wastes as degradation products of more complex organic compounds whose complexation with actinides has a direct impact on the behavior of actinides in waste storage and processing. Other ligands may not exist in nuclear wastes, but they are members of a series of structurally related ligands to allow a systematic study to help reveal the structure–function relationship. In this work, the complexation of U^{VI} with thiodiacetate was studied at 10 to 85 °C. This system has been previously studied at 25 °C,[10,11] but not at elevated temperatures. Furthermore, due to the unavailability of tech-

[a] Dipartimento di Scienze Chimiche, Università di Padova, via Marzolo 1, 35131 Padova, Italy
Fax: +39-049-827-5161,
E-mail: plinio.dibernardo@unipd.it
[b] Istituto di Chimica Inorganica e delle Superfici del C.N.R. of Padova,
Corso Stati Uniti 4, 35127, Padova, Italy
[c] Chemical Sciences Division, Lawrence Berkeley National Laboratory,
Berkeley, CA 94720, U.S.A.
Fax: +1-510-486-5596,
E-mail: lrao@lbl.gov

Supporting information for this article is available on the WWW under http://www.eurjic.org or from the author.

niques to characterize the coordination modes, no structural information on the U^{VI}-thiodiacetate complexes in solution was obtained in the earlier studies. Therefore, the primary objectives in this work are: (1) to extend the thermodynamic database for the complexation of U^{VI} with thiodiacetate to elevated temperatures; (2) to gain insight into the energetics of the complexation and the effect of temperature; and (3) to establish the coordination modes in the complexes. Thermodynamic parameters, including formation constants, enthalpy, and entropy, were determined by potentiometry and calorimetry. EXAFS was used, in conjunction with the thermodynamic data, to establish the coordination modes in the complexes.

Results and Discussion

Protonation of Thiodiacetate at 10–85 °C

The protonation constants of thiodiacetate at different temperatures were calculated from the data obtained by potentiometry. These constants were then used in the calculation of the enthalpies of protonation from the data obtained by calorimetry at the same temperature. The results are summarized in Table 1. The values obtained at 25 °C are in good agreement with the values at 20 and 25 °C in the literature.[10,12]

As is typical of many carboxylic acids,[13] the enthalpies of protonation of thiodiacetate are small (a few kilojoules per mol) and become more endothermic when the temperature is increased (Table 1). On the other hand, the entropy of protonation increases from 76 $J K^{-1} mol^{-1}$ (10 °C) to 100 $J K^{-1} mol^{-1}$ (85 °C) for HL, and from 130 $J K^{-1} mol^{-1}$ (10 °C) to 172 $J K^{-1} mol^{-1}$ (85 °C) for H_2L, thus favoring the protonation at higher temperatures. The increase in the entropy term ($T\Delta S$) is slightly larger than the increase in the enthalpy, which results in a net increase in the protonation constants when the temperature is increased.

Comparison between the thermodynamic functions concerning the protonation reactions of TDA^{2-} and ODA^{2-} may give additional information about these species in solution. Figure 1 shows the entropy and enthalpy of the first protonation of TDA^{2-} and ODA^{2-} ($H + L^{2-} \leftrightharpoons HL^-$) at different temperatures. The entropies of protonation of TDA^{2-} and ODA^{2-} are almost identical in the entire temperature region, whereas the enthalpies of protonation of TDA^{2-} and ODA^{2-} are parallel to each other, with a constant difference of 1.5 $kJ mol^{-1}$, at any given temperature. The fact that the $T\Delta S$ terms for TDA^{2-} and ODA^{2-} are identical at any temperature implies that the same degree of

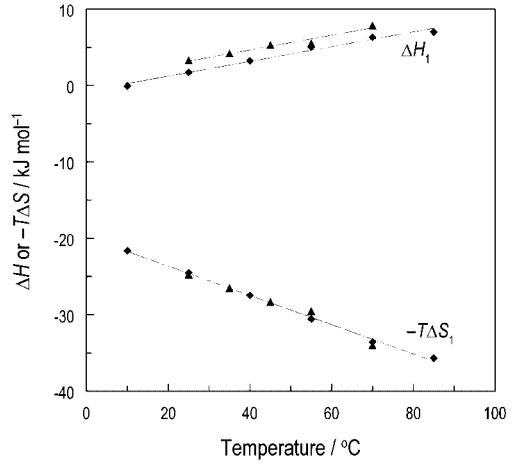

Figure 1. The thermodynamic parameters for the first protonation reaction of thiodiacetate (♦) and oxydiacetate (▲).[9] I = 1.05 $mol kg^{-1}$ $NaClO_4$.

Table 1. Protonation of thiodiacetate (I = 1.05 $mol kg^{-1}$ $NaClO_4$); the error limits represent 3σ.

	T [°C]	$\log\beta_{H,M}$	$\log\beta_{H,m}$	$-\Delta G$ [$kJ mol^{-1}$]	ΔH [$kJ mol^{-1}$]	ΔS [$J K^{-1} mol^{-1}$]	Ref.
$H^+ + L^{2-} \leftrightharpoons HL^-$	10	4.02 ± 0.02	4.00 ± 0.02	21.68 ± 0.11	–(0.05 ± 0.03)	76.4 ± 0.4	
	20	4.04 ± 0.02					[10]
	25	4.01 ± 0.02	3.99 ± 0.02	22.77 ± 0.11	1.73 ± 0.06	82.2 ± 0.4	
		3.99 ± 0.01			1.82 ± 0.11		[12]
	40	4.06 ± 0.03	4.04 ± 0.03	24.22 ± 0.18	3.24 ± 0.09	87.7 ± 0.6	
	55	4.08 ± 0.01	4.06 ± 0.01	25.50 ± 0.06	5.05 ± 0.15	93.1 ± 0.5	
	70	4.17 ± 0.01	4.15 ± 0.01	27.26 ± 0.07	6.3 ± 0.4	97.8 ± 1.2	
	85	4.20 ± 0.01	4.18 ± 0.01	28.66 ± 0.07	7.0 ± 0.3	99.6 ± 0.9	
$2 H^+ + L^{2-} \leftrightharpoons H_2L$	10	7.21 ± 0.02	7.17 ± 0.02	38.87 ± 0.11	–(2.16 ± 0.03)	129.6 ± 0.4	
	20	7.18 ± 0.02					[10]
	25	7.21 ± 0.02	7.17 ± 0.02	40.92 ± 0.11	1.13 ± 0.10	141.0 ± 0.5	
		7.13 ± 0.01			1.36 ± 0.15		[12]
	40	7.25 ± 0.02	7.21 ± 0.02	43.22 ± 0.12	3.84 ± 0.07	150.3 ± 0.4	
	55	7.28 ± 0.01	7.24 ± 0.01	45.48 ± 0.06	6.96 ± 0.27	159.8 ± 0.8	
	70	7.39 ± 0.01	7.35 ± 0.01	48.28 ± 0.07	9.3 ± 0.7	167.8 ± 2.0	
	85	7.40 ± 0.01	7.36 ± 0.01	50.46 ± 0.07	11.0 ± 0.3	171.6 ± 0.9	
$H^+ + OH^- \leftrightharpoons H_2O$	10	14.46 ± 0.01			–58.75		
	25	13.78 ± 0.01			–56.27		
	40	13.20 ± 0.01			–52.99		
	55	12.88 ± 0.06			–50.8		
	70	12.54 ± 0.01			–48.6		
	85	12.10 ± 0.10			–45.3		

disorder is generated when these two doubly charged anions are protonated. The fact that the enthalpy of protonation of ODA^{2-} is higher than that of TDA^{2-} at all temperatures probably results from the lower basicity of ODA^{2-} than TDA^{2-}, which is due to a higher inductive effect exerted by the ether oxygen in ODA^{2-} than the sulfur in TDA^{2-}. Since this inductive effect is likely to be independent of temperature, the difference in the enthalpies of protonation for TDA^{2-} and ODA^{2-} remains constant (approx. 1.5 kJ mol^{-1}) at any temperature and parallel trends in the enthalpy are observed.

Complexation of Uranium(VI) with Thiodiacetate

Stability Constants at 10–85 °C

Two representative potentiometric titrations at 10 and 85 °C are shown in Figure 2. The best model to fit the potentiometric data in the entire temperature range includes the formation of three U^{VI}/TDA complexes (ML, MHL, and MHL_2):

$UO_2^{2+} + L^{2-} \leftrightharpoons UO_2L(aq)$

$UO_2^{2+} + H^+ + L^{2-} \leftrightharpoons UO_2HL^+$

$UO_2^{2+} + H^+ + 2L^{2-} \leftrightharpoons UO_2HL_2^-$

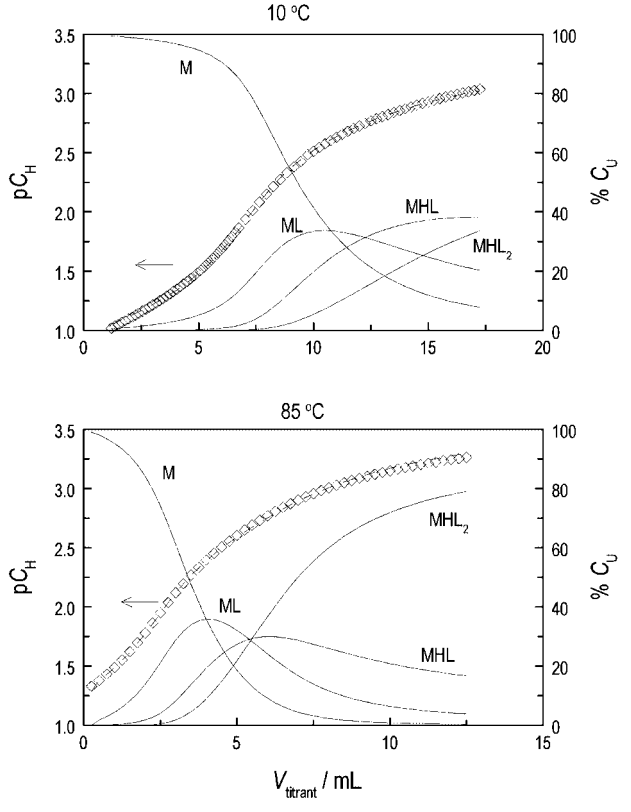

Figure 2. Potentiometric titrations of U^{VI}/thiodiacetate complexation. I = 1.05 mol kg^{-1} $NaClO_4$. Top: T = 10 °C; V^0 = 32.0 cm^3, C_H^0 = 110.0 mM, C_U^0 = 19.22 mM; titrant C_H/C_{TDA} = 0.485:0.481 M. Bottom: T = 85 °C; V^0 = 29.0 cm^3, C_H^0 = 51.35 mM, C_U^0 = 21.19 mM; titrant C_H/C_{TDA} = 0.556:0.556 M. Symbols: ◊: experimental data (pC_H); dashed curve: fit (pC_H); solid lines: percentage of U^{VI} species (right y axis).

The formation constants and Gibbs free energy of complexation at different temperatures were calculated and are given in Table 2. The model developed for the entire temperature range (from 10 to 85 °C) from this study is identical to the model for 25 °C from a previous study,[11] and the values at 25 °C from both studies agree well (Table 2). The data from this work indicate that the complexation between uranium(VI) and thiodiacetate is enhanced at elevated temperatures. The ML, MHL, and MHL_2 complexes at 85 °C are 6, 5, and 40 times as strong as those at 10 °C, respectively. The enhancement of complexation at elevated temperatures is consistent with the predictions by a simple electrostatic model that was developed to interpret the effect of temperature on the formation of lanthanide and actinide carboxylate complexes.[6–9,14]

Enthalpy and Entropy of Complexation at 10–85 °C

A representative set of four calorimetric titrations at 25 °C is shown in part a of Figure 3. Similar titrations with solutions of different concentrations (C_U and C_H) were performed at 10, 40, 55, 70, and 85 °C (see Table S3 in the Supporting Information). Using the formation constants of the complexes calculated from potentiometry, in conjunction with the constants and enthalpies of protonation (Table 1), the enthalpies of complexation for ML, MHL, and MHL_2 were calculated from the calorimetric titration data (see Table 2).

Using the thermodynamic values for protonation and complexation in Tables 1 and 2, simulated calorimetric titration curves for 10, 40, and 85 °C were calculated (Figure 3, b). The excellent agreement between the curves and experimental points confirms the mutual consistency of the calorimetric and potentiometric data on the complexation as well as the reliability of the data on protonation.

The data in Table 2 show that, as the temperature is increased, both the enthalpy and entropy of complexation increase, making opposite contributions to the temperature effect on the Gibbs free energy (and thus on the overall stability of the complexes). The overall stability constants increase because the increase in the entropy term ($T\Delta S$) exceeds the increase in the enthalpy. These trends are similar to previous observations for the U^{VI}/acetate,[7] U^{VI}/malonate,[8] and U^{VI}/oxydiacetate[9] systems, and are expected for typical hard acid–hard base interactions.[3] The increase of entropy with temperature could be the consequence of a more disordered bulk water structure due to the perturbation by more thermal motion at higher temperatures. In the process of complexation, the solvating water molecules are released to a more disordered bulk solvent. As a result, the gain in the complexation entropy is larger at higher temperatures. Meanwhile, the released water molecules would form fewer and/or weaker hydrogen bonds with the bulk water due to the thermal motion, thus resulting in less favorable enthalpy of complexation at higher temperatures. Detailed discussions on this point are given elsewhere.[6–9,14]

Figure 4 shows that the molar enthalpies of complexation for the three complexes increase monotonously as the temperature is increased. From these data, the heat capacity

Table 2. Complexation of U^{VI} with thiodiacetate (I = 1.05 mol kg^{-1} $NaClO_4$); the error limits represent 3σ.

	T [°C]	$\log\beta_M$	$\log\beta_m$	$-\Delta G$ [kJ mol^{-1}]	ΔH [kJ mol^{-1}]	ΔS [J K^{-1} mol^{-1}]	Ref.
$UO_2^{2+} + L^{2-} \leftrightharpoons UO_2L(aq)$	10	2.91 ± 0.03	2.89 ± 0.03	15.67 ± 0.16	13.4 ± 0.4	102.6 ± 1.5	
	20	3.16 ± 0.03					[10]
	25	3.04 ± 0.03	3.02 ± 0.03	17.24 ± 0.17	15.7 ± 0.7	110.5 ± 2.4	
		2.97 ± 0.02			14.8 ± 0.2		[11]
	40	3.23 ± 0.03	3.21 ± 0.03	19.24 ± 0.18	16.3 ± 0.9	113.5 ± 2.9	
	55	3.35 ± 0.05	3.33 ± 0.05	20.9 ± 0.3	19.2 ± 1.2	122.3 ± 3.8	
	70	3.62 ± 0.03	3.60 ± 0.03	23.65 ± 0.20	20.5 ± 1.8	129 ± 5	
	85	3.68 ± 0.05	3.66 ± 0.05	25.1 ± 0.3	23.0 ± 1.8	134 ± 5	
$UO_2^{2+} + H^+ + L^{2-} \leftrightharpoons UO_2HL^+$	10	5.66 ± 0.04	5.62 ± 0.04	30.46 ± 0.22	7.5 ± 0.6	134.1 ± 2.2	
	25	5.76 ± 0.06	5.72 ± 0.06	32.6 ± 0.3	11.9 ± 1.2	150 ± 4	
		5.43 ± 0.10			17.8 ± 0.4		[11]
	40	5.63 ± 0.07	5.59 ± 0.07	33.5 ± 0.4	27 ± 4	193 ± 13	
	55	5.98 ± 0.07	5.94 ± 0.07	37.3 ± 0.4	21.4 ± 2.1	179 ± 6	
	70	6.10 ± 0.08	6.06 ± 0.08	39.8 ± 0.5	25 ± 3	189 ± 9	
	85	6.34 ± 0.08	6.30 ± 0.08	43.2 ± 0.6	30.3 ± 2.7	205 ± 8	
$UO_2^{2+} + H^+ + 2L^{2-} \leftrightharpoons UO_2HL_2^-$	10	8.10 ± 0.08	8.04 ± 0.08	43.6 ± 0.4	24.3 ± 0.6	239.7 ± 2.6	
	20	8.42 ± 0.06					[10]
	25	8.48 ± 0.07	8.42 ± 0.07	48.1 ± 0.4	30.0 ± 1.2	262 ± 4	
		8.39 ± 0.11			25.7 ± 0.2		[11]
	40	8.70 ± 0.07	8.64 ± 0.07	51.8 ± 0.4	38.6 ± 3.6	289 ± 12	
	55	9.03 ± 0.07	8.97 ± 0.07	56.4 ± 0.4	38.0 ± 1.5	288 ± 5	
	70	9.36 ± 0.07	9.30 ± 0.07	61.1 ± 0.5	39.0 ± 2.5	292 ± 7	
	85	9.69 ± 0.08	9.63 ± 0.08	66.0 ± 0.6	38.2 ± 2.4	291 ± 7	

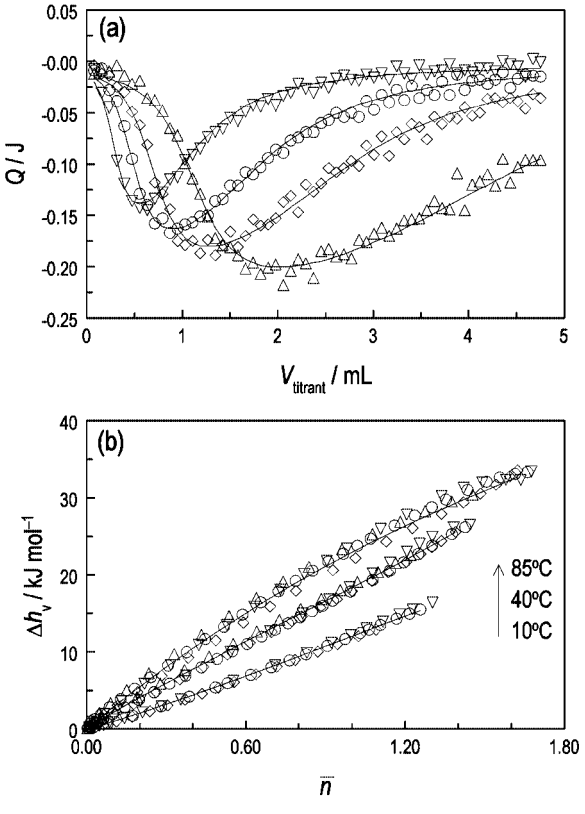

Figure 3. Calorimetric titrations of the uranium(VI) thiodiacetate system. I = 1.05 mol kg^{-1} $NaClO_4$. (a) Q vs. $V_{titrant}$ at 25 °C, four titrations with different C_M and C_H; (b) Δh_v vs. $\bar{n}$ at 10, 40, and 85 °C; three or four titrations with different C_M and C_H were conducted at each temperature. The number of points in the figure has been reduced for clarity. Detailed conditions for ◊, ○, △, and ▽ are given in Table S3 of the Supporting Information.

of complexation, $\Delta C_p°$, was calculated to be 122 ± 16, 302 ± 26, and 242 ± 23 J K^{-1} mol^{-1} for UO_2L, UO_2HL^+, and $UO_2HL_2^-$, respectively.

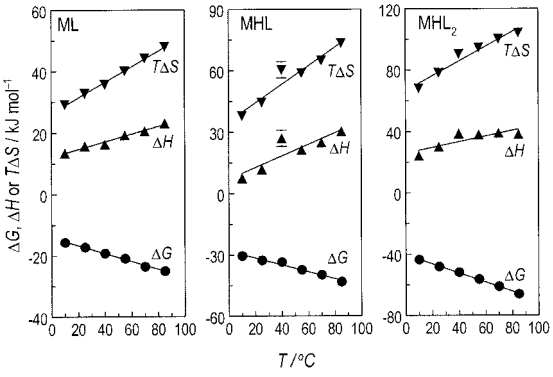

Figure 4. Overall thermodynamic parameters for the complexation of U^{VI} with thiodiacetate. I = 1.05 mol kg^{-1} $NaClO_4$.

Coordination Modes

The results of EXAFS experiments with three U^{VI} solutions are shown in Figure 5 and Table 3. Solution I contains 100% free UO_2^{2+}. Speciation calculations with the stability constants in Table 2 indicate that the major species in solution II are UO_2HL^+ (51%) and free UO_2^{2+} (30%), while the major species in solution III is $UO_2HL_2^-$ (86%). The FT magnitudes for solutions I and II are quite similar and are fitted with two U–O scattering paths at 1.77–1.78 Å and five U–O scattering paths at 2.40–2.41 Å. The two oxygens at 1.77–1.78 Å are the axial oxygens in the UO_2^{2+} moiety and the five oxygens at 2.40–2.41 Å are from the water and/or the thiodiacetate ligands in the equatorial plane of

Table 3. Fitting parameters for uranium L_{III}-edge EXAFS.

Samples	Shell	R[a] [Å]	N[a]	σ[b] [Å]	ΔE_0 [eV]
Solution I[c]	$U–O_{ax}$	0.77	1.8	0.0385	–13.69
(0.02 M U^{VI}/0.1 M $HClO_4$)	$U–O_{eq}$	2.41	5.5	0.0871	–13.69
Solution II	$U–O_{ax}$	0.78	2.0	0.0531	–13.77
(0.02 M U^{VI}/0.5 M TDA, pH 2.0)	$U–O_{eq}$	2.40	5.4	0.1040	–13.77
Solution III	$U–O_{ax}$	0.79	2.0	0.0526	–16.58
(0.02 M U^{VI}/0.5 M TDA, pH 3.5)	$U–O_{eq1}$	2.34	1.7	0.0368	–16.58
	$U–O_{eq2}$	2.49	2.7	0.0573	–16.58

[a] The 95% confidence limits for the bond lengths (R) and coordination numbers (N) for each shell are: $U–O_{ax}$ = 0.01 Å and ±15%; $U–O_{eq}$ = 0.02 Å and ±25%, respectively. [b] σ is the EXAFS Debye–Waller term which accounts for the effects of thermal and static disorder through damping of the EXAFS oscillations by the factor $\exp(-2k^2\sigma^2)$. [c] Data from ref.[8]

UO_2^{2+}. The FT magnitude for solution III shows, besides the prominent peak for the two axial oxygens, two distinct shells in the range of 1.7–2.3 Å (phase shift not corrected) and is fitted with two U–O scattering paths at 2.34 Å and three U–O scattering paths at 2.49 Å. In the following discussion, these structural data are used in conjunction with the thermodynamic parameters of complexation to shed light on the coordination modes in the UO_2L, UO_2HL^+, and $UO_2HL_2^-$ complexes.

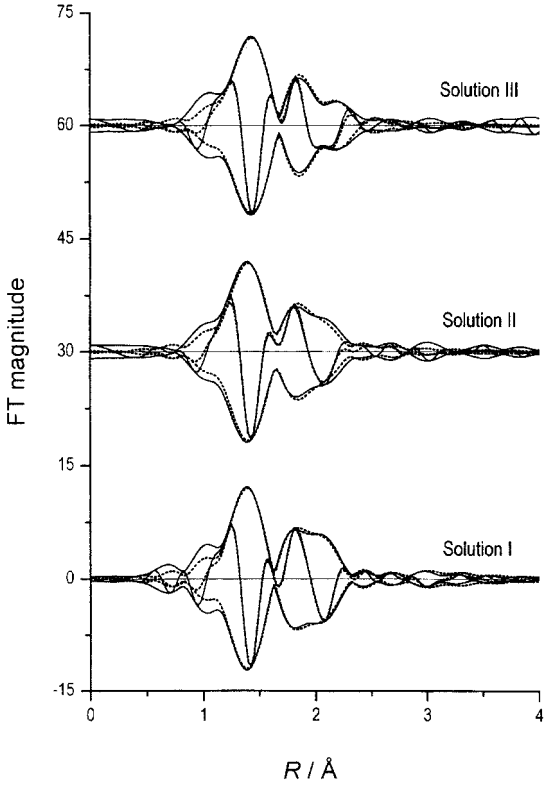

Figure 5. Fourier (FT) transform magnitude $\chi(k)\times k^3$ of the uranium L_{III}-edge EXAFS. Solid lines: experimental, dotted lines: fitted. Fitting results are given in Table 3.

$UO_2HL_2^-$

Because this species is dominant (86%) in solution III, it is possible to propose a structure for this species based on the EXAFS data. In this complex, one TDA is fully deprotonated (L^{2-}) and the other TDA ligand is partially protonated (HL^-). As discussed in a previous study for the complexation of U^{VI} with oxydiacetate (ODA),[9] the partially protonated ligand (HL^-) is likely to prefer a "terminal" didentate coordination mode in the complex, leaving the protonated carboxylate group free from metal binding. A proposed structure of the $UO_2HL_2^-$ complex is shown in Figure 6 (a), where one TDA (L^{2-}) is coordinated with U^{VI} in a "global" didentate mode while the other TDA (HL^-) is in a "terminal" didentate mode similar to that in the uranium(VI) acetate complex described in the literature.[7] The U–O distance in the "global" didentate mode is shorter (2.34 Å) than that in the "terminal" didentate mode (2.49 Å). The oxygen from the water molecule is at a similar distance to the two oxygens of the "terminal" didentate carboxylate group and is not resolved by EXAFS.

UO_2HL^+

Solution II contains 51% UO_2HL^+ and 30% free UO_2^{2+} (30%). Therefore, the EXAFS data reflect the average coordination of U^{VI} in these two major species. Because the partially protonated TDA ligand (HL^-) is likely to take a "terminal" didentate coordination mode in the complex, the structure of the UO_2HL^+ complex is proposed as shown in Figure 6 (b). The two oxygens from the terminal carboxylate group and the three oxygens from water molecules are all around 2.40 Å, resulting in a similar coordination shell of five oxygens as in the free $UO_2(H_2O)_5^{2+}$ (Solution I).

UO_2L

This complex is not a major species in either solution I or solution II. Therefore, the EXFAS data do not provide information on the coordination mode of TDA in this complex. However, based on the structures of $UO_2HL_2^-$ (Figure 6, a) and UO_2HL^+ (Figure 6, b) proposed from the EXFAS data, it is reasonable to assume that the sulfur atom in UO_2L does not participate in bonding with U^{VI}. Moreover, since the entropy of complexation primarily reflects the effect of dehydration and chelate formation, comparison of the entropy of complexation between TDA and structurally related dicarboxylates (e.g., ODA) could help reveal the coordination mode(s). A previous study has shown that, at 25 °C, one carboxylate group contributes approximately 50 $J\,K^{-1}\,mol^{-1}$ to the overall entropy of complexation.[9] For example, the value of ΔS_{298} for the didentate U^{VI}–phenylene-1,2-dioxydiacetate complex is 103 $J\,K^{-1}\,mol^{-1}$, while the values of ΔS_{298} for the tridentate U^{VI}–oxydiacetate and

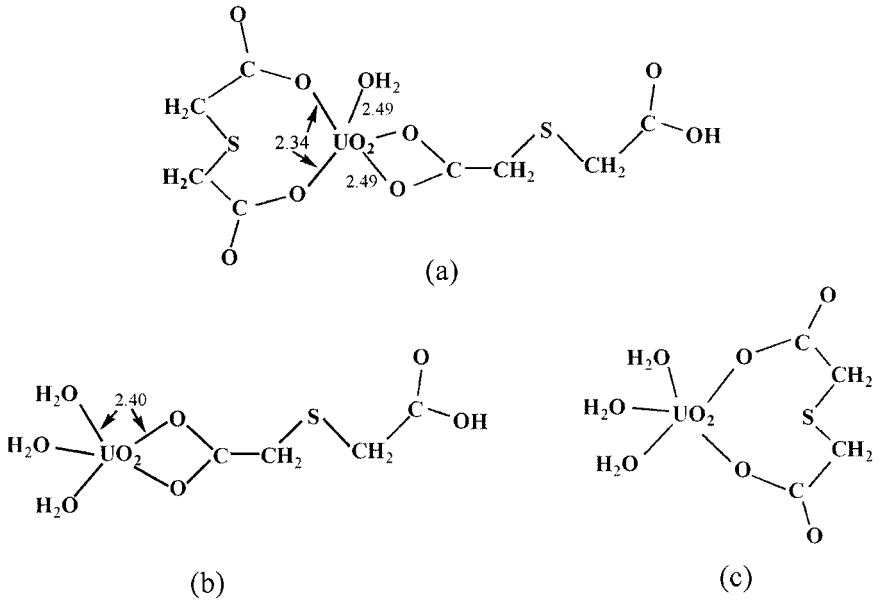

Figure 6. Proposed structures of uranium(VI) thiodiacetate complexes in solution: (a) $UO_2HL_2^-$, (b) UO_2HL^+, (c) UO_2L(aq), where L^{2-} stands for the thiodiacetate anion.

U^{VI}–iminodiacetate complexes are 152 and 161 $J\,K^{-1}\,mol^{-1}$, respectively. The oxydiacetate and iminodiacetate ligands in these complexes are tridentate because the ether oxygen or the nitrogen atoms participate in the complexation.[9] The value of ΔS_{298} for the U^{VI}-TDA complex (UO_2L) is 110 $J\,K^{-1}\,mol^{-1}$ from this work (Table 2), similar to that for the didentate U^{VI}–phenylene-1,2-dioxydiacetate complex but much smaller than those for the tridentate U^{VI}-ODA and U^{VI}-IDA complexes. Thus, the thermodynamic data are consistent with a didentate mode in the 1:1 U^{VI}-TDA complex. Both carboxylate groups of TDA coordinate with U^{VI} while the sulfur atom does not participate in the complexation. A proposed structure for UO_2L is shown in Figure 6 (c).

Conclusions

In the temperature range from 10 to 85 °C, three uranium(VI) thiodiacetate complexes (UO_2L, UO_2HL^+, and $UO_2HL_2^-$) have been identified by potentiometry and calorimetry. Both the enthalpy and entropy of complexation increase as the temperature is increased, although they make opposite contributions to the overall stability of the complexes. The complexes become stronger at higher temperatures due to a larger contribution from the entropy, which exceeds the unfavorable effect of enthalpy. The thermodynamic parameters, in conjunction with the structural information from EXAFS, suggest that TDA coordinates with U^{VI} through the carboxylate group(s) and that the sulfur atom does not participate in the complexation. In UO_2L, the fully deprotonated TDA is in a "global" didentate mode through both carboxylate groups. However, in UO_2HL^+ and $UO_2HL_2^-$, the partially protonated TDA is probably in a "terminal" didentate mode, with the protonated carboxylate group free from metal bonding.

Experimental Section

Chemicals: All chemicals were reagent grade or higher. Distilled and deionized water was used in preparations of all the solutions. The stock solution of uranium(VI) perchlorate was prepared by dissolving uranium trioxide (UO_3) in perchloric acid. The concentration of uranium(VI) in the stock solution was determined by absorption spectrophotometry and fluorimetry.[15] Gran's potentiometric method[16] was used to determine the concentration of perchloric acid in the stock solution. Volumetric standard sodium hydroxide solutions were purchased from Brinkmann Instruments, Inc. or Sigma–Aldrich, Inc. and verified to be carbonate-free prior to use. Solutions of sodium thiodiacetate were prepared by adding calculated amounts of sodium hydroxide to solutions of thiodiacetic acid. The ionic strength of all the solutions used in potentiometry and calorimetry was adjusted to 1.0 M at 25 °C by adding appropriate amounts of sodium perchlorate as the background electrolyte.

Potentiometry: The protonation constants of thiodiacetate (TDA) and the stability constants of the uranium(VI) TDA complexes were determined by potentiometric titrations in a temperature range from 10 to 85 °C. A specially designed titration vessel was used to avoid the problem of water condensation during the titrations at temperatures above the ambient. Details of the titration setup have been provided elsewhere.[6]

Electromotive force (EMF, in millivolts) was measured with a Metrohm pH meter (Model 713) equipped with a Ross combination pH electrode (Orion Model 8102). Because potassium perchlorate is much less soluble than sodium perchlorate, precipitation of the former could result in the clogging of the electrode frit glass septum. As a result, the original electrode filling solution (3.0 M potassium chloride) was replaced with 1.0 M sodium chloride. The electrode potential (mV) in acidic solutions can be expressed as Equation (1).

$$E = E^0 + RT/F \ln[H^+] + \gamma_H[H^+] \quad (1)$$

R is the gas constant, F is the Faraday constant, and T is the temperature in Kelvin. The last term in Equation (1), $\gamma_H[H^+]$, is the

electrode junction potential for the hydrogen ion. Prior to each protonation or complexation titration, an acid/base titration with standard perchloric acid and sodium hydroxide solutions was performed to obtain the parameters E^0 and γ_H. These parameters allowed the calculation of hydrogen ion concentrations from the electrode potential in the subsequent titration. Corrections for the electrode junction potential for the hydroxide ion are not necessary in this work because all the experiments were conducted in acidic solutions, where the junction potential for the hydroxide ion is negligible.

Detailed conditions for the potentiometric titrations are provided in Tables S1 and Table S2 in the Supporting Information. Multiple titrations were conducted at each temperature with solutions of different concentrations (C_{TDA}, C_H, and C_U). 50–70 Data points were collected in each titration. The protonation constants of TDA, $K_{H,M}$, and the formation constants of U^{VI}-TDA complexes, $\beta_{j,M}$, on the molarity scale were calculated with the program Hyperquad.[17] To allow the comparison at different temperatures, the constants in molarity were converted into the constants in molality according to Equation (2).[18]

$$\log_{10}K_m = \log_{10}K_M + \Sigma_r v_r \log_{10}\vartheta \quad (2)$$

K_m and K_M are the equilibrium constants of a reaction in molality and molarity, respectively, ϑ is the ratio of the values of molality to molarity for the specific ionic medium. For the 1.0 M $NaClO_4$ used in this study, ϑ equals 1.05 L of solution per kilogram of water. $\Sigma_r v_r$ is the sum of stoichiometric coefficients of the reaction (v_r is positive for products and negative for reactants.)

Calorimetry: Calorimetry was used to determine the enthalpy of thiodiacetate protonation and complexation with U^{VI}. The calorimetric titrations were conducted with both an isoperibol calorimeter (Model ISC-4285, Calorimetry Sciences Corp.) at the Lawrence Berkeley National Laboratory (for T from 25 to 85 °C) and an isothermal microcalorimeter (Thermometric 2277 Thermal Activity Monitor, nanoWatt model) at the University of Padova (for T = 10 °C). The performance of the isoperibol calorimeter was tested by measuring the enthalpy of protonation of 2-bis(2-hydroxyethyl)amino-2-(hydroxymethyl)propane-1,3-diol at different temperatures. The results are –29.1 ± 0.3 kJ mol^{-1} at 45 °C and –29.3 ± 0.3 kJ mol^{-1} at 70 °C, in good agreement with those in the literature (–28.4 ± 0.3 kJ mol^{-1} at 45 °C and –29.3 ± 0.2 kJ mol^{-1} at 70 °C).[19]

Detailed conditions for the calorimetric titrations are provided in Table S3 in the Supporting Information. Multiple titrations were performed at each temperature to obtain the enthalpy of protonation of TDA and the enthalpy of complexation between U^{VI} and TDA, using different concentrations of the titrant or $UO_2(ClO_4)_2$ and $HClO_4$ in the cell. For each titration run, n experimental values of the total heat produced in the reaction vessel ($Q_{ex,j}$, j = 1 to n, usually n = 50–70), were calculated as a function of the volume of the added titrant. These values, corrected for the heat of dilution of the titrant ($Q_{dil,j}$, determined in separate runs), gave the net reaction heat: $Q_{r,j} = Q_{exp,j} - Q_{dil,j}$. A quantity, Δh_v, was then calculated for the stepwise addition by Equation (3).

$$\Delta h_v = \sum_{j=1}^{j=n} (Q_{r,j} - Q_{p,j})/n \quad (3)$$

For the protonation titrations, $Q_{p,j}$ is the heat of water formation and n is the number of mols of TDA in the cell. For the complexation titrations, $Q_{p,j}$ is the sum of the heat calculated for the water formation and ligand protonation while n is the number of mols of U^{VI} in the cell. The enthalpies of reaction were calculated, with a home modified version of the computer program Letagrop,[20] to use Δh_v as the error-carrying variable while assigning equal weight to all the titrations with different amounts of uranium(VI) (for the U/TDA systems) or TDA (for the H/TDA systems).

EXAFS Spectroscopy: Three uranium(VI) solutions were prepared for EXAFS experiments. Solution I contained 0.02 M $UO_2(ClO_4)_2$ in 0.1 M $HClO_4$ with no thiodiacetic acid. Solutions II and III contained 0.02 M $UO_2(ClO_4)_2$ and 0.5 M thiodiacetic acid at pH 2.0 and 3.5, respectively. Approximately 2 mL of each solution was sealed in a polyethylene tube (5 mm i.d.) and mounted on an aluminum sample positioner with Scotch tape for the experiments.

Uranium L_{III}-edge EXAFS spectra were collected at the Stanford Synchrotron Radiation Laboratory (SSRL) on beamline 4-1 under normal ring operating conditions (3.0 GeV, 50–100 mA). Energy scans of the polychromatic X-ray beam were obtained using a Si(220) double-crystal monochromator. The vertical slit width was 0.5 mm, which reduced the effects of beam instabilities and monochromator glitches while providing ample photon flux. The higher order harmonic content of the beam was reduced by detuning the crystals in the monochromator so that the incident flux was reduced to 50% of its maximum at the scan ending energy. The EXAFS data were collected in both the transmission mode using argon-filled ionization chambers and the fluorescence mode using a four-element Ge detector, up to $k_{max} \approx 15$ Å^{-1}. Usually three or four scans were performed for each sample. Energy calibration was based on assigning the first inflection point of the absorption edge for uranium dioxide to 17166 eV. The EXAFS spectra were fitted with the R-space X-ray Absorption Package (RSXAP),[21] using parameterized phase and amplitude functions generated by the program FEFF7.[22] Single scattering interactions of U–O_{ax} (axial oxygen) and U–O_{eq} (equatorial oxygen) were included.

Supporting Information (see footnote on the first page of this article): Tables S1 and S2: Experimental conditions of potentiometry for proton/thiodiacetate and uranium(VI)/thiodiacetate systems, respectively. Table S3. Experimental conditions of calorimetry for thiodiacetate protonation and uranium(VI)/thiodiacetate complexation.

Acknowledgments

This work was supported by the Director, Office of Science, Office of Basic Energy Sciences, Division of Chemical Sciences, under U.S. Department of Energy Contract No. DE-AC02-05CH11231 at Lawrence Berkeley National Laboratory and by the Ministero dell'Università e della Ricerca Scientifica e Tecnologica (MURST, Roma) within the program COFIN02. The EXAFS experiments were conducted at SSRL, which is operated by the Department of Energy, Division of Chemical Sciences.

[1] E. Martell, R. M. Smith, *Critical Stability Constants*, vol. 3, Plenum Press, New York, **1977**; first suppl., **1982**; second suppl., **1989**.

[2] T. M. Seward, *Metal Complex Formation in Aqueous Solutions at Elevated Temperatures and Pressures*, in *Chemistry and Geochemistry of Solutions at High Temperatures and Pressures*, Physics and Chemistry of the Earth, volumes 13 and 14 (Eds.: D. T. Rickard, F. E. Wickman), Pergamon Press, New York, **1981**, 113–128.

[3] E. N. Rizkalla, G. R. Choppin, *Lanthanides and Actinides Hydration and Hydrolysis*, in *Handbook on the Physics and Chem-*

istry of Rare Earths, vol. 18, *Lanthanides/Actinides: Chemistry* (Eds.: K. A. Gschneider Jr, L. Eyring, G. R. Choppin, G. H. Lander), Elsevier Science B. V., New York, **1994**.
[4] D. A. Wruck, P. Zhao, C. E. A. Palmer, R. J. Silva, *J. Solution Chem.* **1997**, *26*, 267–275.
[5] S. A. Wood, D. J. Wesolowski, D. A. Palmer, *Chem. Geol.* **2000**, *167*, 231–253.
[6] P. Zanonato, P. Di Bernardo, A. Bismondo, L. Rao, G. R. Choppin, *J. Solution Chem.* **2001**, *30*, 1–18.
[7] J. Jiang, L. Rao, P. Di Bernardo, P. Zanonato, A. Bismondo, *J. Chem. Soc., Dalton Trans.* **2002**, 1832–1836.
[8] L. Rao, J. Jiang, P. Zanonato, P. Di Bernardo, A. Bismondo, A. Y. Garnov, *Radiochim. Acta* **2002**, *90*, 581–588.
[9] L. Rao, A. Yu. Garnov, J. Jiang, P. Di Bernardo, P. Zanonato, A. Bismondo, *Inorg. Chem.* **2003**, *42*, 3685–3692.
[10] A. Cassol, P. Di Bernardo, R. Portanova, L. Magon, *Inorg. Chim. Acta* **1973**, *7*, 353–358.
[11] P. Di Bernardo, G. Tomat, A. Bismondo, O. Traverso, L. Magon, *J. Chem. Res. (M)* **1980**, 3144–3171.
[12] I. Dellien, I. Grenthe, G. Hessler, *Acta Chem. Scand.* **1973**, *27*, 2431–2440.
[13] A. E. Martell and R. M. Smith, *Critical Stability Constants*, vol. 6, Plenum Press, New York, **1989**.
[14] L. Rao, Z. C. Zhang, P. Zanonato, P. Di Bernardo, A. Bismondo, S. B. Clark, *Dalton Trans.* **2004**, 2867–2872.
[15] C. W. Sill, H. E. Peterson, *Anal. Chem.* **1947**, *19*, 646–651.
[16] G. Gran, *Analyst* **1952**, *77*, 661–671.
[17] P. Gans, A. Sabatini, A. Vacca, *Talanta* **1996**, *43*, 1739–1753.
[18] W. Hummel, G. Anderegg, I. Puigdomenech, L. Rao, O. Tochiyama; *Chemical Thermodynamics of Compounds and Complexes of U, Np, Pu, Am, Tc, Zr, Ni, and Se with Selected Organic Ligands* (Eds.: F. J. Mompean, M. Illemassène, J. Perrone), Elsevier Science B. V., Amsterdam, **2005**.
[19] R. Smith, P. Zanonato, G. R. Choppin, *J. Chem. Thermodyn.* **1992**, *24*, 99–106.
[20] R. Arnek, *Arkiv Kemi* **1970**, *32*, 81.
[21] B. J. E. Penner-Hahn, *Coord. Chem. Rev.* **1999**, *190–192*, 1101–1123.
[22] http://lise.lbl.gov/RSXAP.

Received: June 15, 2006
Published Online: September 20, 2006

